

Towards polarization-enhanced PET:  
Study of random background in  
polarization-correlated Compton events

Ana Marija Kožuljević<sup>1,2</sup>, Tomislav Bokulić<sup>1</sup>, Darko Grošev<sup>3</sup>,  
Siddharth Parashari<sup>4</sup>, Luka Pavelić<sup>2</sup>, Marinko Rade<sup>5,6,7</sup>, Marijan  
Žuvić<sup>3</sup>, and Mihael Makek<sup>1</sup>

<sup>1</sup>University of Zagreb, Faculty of Science, Zagreb, Croatia

<sup>2</sup>Institute for Medical Research and Occupational Health, Zagreb,  
Croatia

<sup>3</sup>University Hospital Centre Zagreb, Zagreb, Croatia

<sup>4</sup>Instituto de Física Corpuscular (IFIC), CSIC-UV, Valencia, Spain

<sup>5</sup>Kuopio University Hospital, University of Eastern Finland,  
Kuopio, Finland

<sup>6</sup>Juraj Dobrila University, Pula, Croatia

<sup>7</sup>Medi-lab d.o.o., Zagreb, Croatia

October 15, 2025

**Abstract**

Positron Emission Tomography (PET) is a medical imaging modality that utilizes positron-emitting isotopes, such as Ga-68 and F-18, for many diagnostic purposes. The positron annihilates with an electron from the surrounding area, creating two photons of 511 keV energy and opposite momenta, entangled in their orthogonal polarizations. When each photon undergoes a Compton scattering process, the difference of their azimuthal scattering angles reflects the initial orthogonality of their polarizations, peaking at  $\pm 90^\circ$ . This type of correlation is not yet utilized in conventional PET scanners, but could potentially offer an energy-independent method for background reduction. Measurements of these kinds of correlations can be achieved using Compton polarimeters, built from a single layer of segmented scintillating crystals such as Gadolinium Aluminium Gallium Garnet doped with Cerium (GAGG:Ce), read out by silicon photomultipliers (SiPMs). In this paper, we study the signal-to-random background ratios in measurements of these correlated annihilation photons from coincidence time spectra across clinically relevant source activities, from  $\sim 200$  MBq to  $\sim 378$  MBq. These are then

---

compared to the standard single-pixel (photoelectric) measurements. We find that the signal-to-random background ratios (SBRs) obtained from the polarization-correlated events for Compton scattering angles  $\theta_{1,2} \in [72^\circ, 90^\circ]$  and azimuthal angle difference  $\Delta\phi \in [70^\circ, 110^\circ]$  are consistently higher than those from single-pixel events, with the ratio of their SBR values of 1.23. The SBR of the selected events also increases with the polarimetric modulation factor  $\mu$ , gaining  $\sim 50\%$  in value during the experiment.

Positron Emission Tomography, quantum entanglement, polarization correlations, annihilation photons, signal to background ratio

## 1 Introduction

Recently, studies investigating possible enhancements of Positron Emission Tomography (PET) imaging turned to the exploration of the positron annihilation process [1, 2, 3]. Quantum mechanics, through energy and spin conservation, necessitates the entanglement of the two photons created in the process [4]—a property not yet utilized in conventional PET scanners, as opposed to their 511 keV energies and opposite momenta. To create a line of response (LOR) through the annihilation site, the two photons originating from it must be detected in coincidence. Since the timing window for coincidences has a finite width, this opens an opportunity for the detection of two photons that are not coming from the same annihilation site, so-called random coincidences. Since the LOR created from these events does not correspond to the annihilation site, the quality of the resulting image is degraded. If the information about the entanglement of the annihilation photons is implemented through the measurement of their polarization correlations, it could be possible to reduce the random background, since it lacks this type of correlation [5, 6, 7, 8, 9].

The polarization correlations of annihilation photons can be measured through the Compton scattering process [4, 10]. If both annihilation photons detected in coincidence undergo Compton scattering in their respective detectors, through measurements of the Compton scattering angle  $\theta$  and azimuthal scattering angle  $\phi$ , it is possible to deduce the azimuthal scattering angle difference  $\Delta\phi$ . The  $\Delta\phi$  values reflect the initial orthogonality of the polarizations (Figure 2), with the highest cross-section for the  $\pm 90^\circ$  difference for fixed values of  $\theta_{1,2}$  [4]:

$$\frac{d^2\sigma}{d\Omega_1 d\Omega_2} = \frac{r_0^4}{16} [F(\theta_1)F(\theta_2) - G(\theta_1)G(\theta_2)\cos(2\Delta\phi)], \quad (1)$$

with  $F(\theta_i) = \frac{[2+(1-\cos\theta_i)^3]}{(2-\cos\theta_i)^3}$  and  $G(\theta_i) = \frac{\sin^2\theta_i}{(2-\cos\theta_i)^2}$ , where  $r_0$  is the classical electron radius,  $d\Omega_{1,2}$  are the solid angles,  $\theta_{1,2}$  are the Compton scattering angles, and  $\Delta\phi = (\phi_1 - \phi_2)$  is the difference of the azimuthal scattering angles of photon 1 and 2, respectively. The polarimetric modulation factor  $\mu$ :

$$\mu = G(\theta_1)G(\theta_2) \quad (2)$$

---

reflects the sensitivity of the detector setup to the initial orthogonality of the polarizations. This factor will have the highest value of  $\sim 42\%$  for  $\theta_{1,2} \approx 82^\circ$  for an ideal detector [7]. The experimentally determined values will always be somewhat lower since the detector acceptance is not perfect, and could depend on the environment in which the positron is emitted [11].

The idea of utilizing these polarization correlations in PET has been investigated *in-silico* [5, 6, 7, 8, 12] and recently been studied through experimental works [9, 13, 14]. There is also an ongoing theoretical discussion about the precise description of the conducted measurements and the nature of the annihilation process [15, 16, 17, 18, 19]. This paper contributes to the line of positron annihilation research by investigating the potential for reducing background in measurements of polarization-correlated annihilation photons at clinically relevant activities for utilization in PET imaging.

## 2 Methods

### 2.1 The detector modules

Two detector modules were assembled from four  $8 \times 8$  matrices of GAGG:Ce crystals, with each crystal sized at  $3 \text{ mm} \times 3 \text{ mm} \times 20 \text{ mm}$ , totaling two  $16 \times 16$  detector matrices with a 3.2 mm matrix pitch. The SiPMs (Hamamatsu Photonics, model S13361-0808A) were glued to the crystals in a one-to-one coupling with optical cement (EJ-500, Eljen Technology, USA). The relative energy resolutions at 511 keV of the two detectors were found to be  $(8.1 \pm 1.1)\%$  and  $(9.3 \pm 2.2)\%$  [20]. The detector modules were mounted on a rotating gantry and arranged so that their faces opposed each other at a distance of 430 mm, with a solution of the Ga-68 source placed between the modules at the center of the gantry's ring (Figure 1).

### 2.2 Data acquisition

Measurements were conducted at the Department of Nuclear Medicine and Radiation Protection, University Hospital Centre Zagreb, with a Ga-68 isotope source at an initial activity of  $\sim 378 \text{ MBq}$ . The read-out and digitization of the data acquired in this setup were performed with the TOFPET2 ASIC system (PETsys Electronics — Medical PET Detectors, S.A., Oeiras, Portugal)[21]. It was set to trigger on coincidences in which at least one pixel fired per module. Each such hit had a timestamp that allowed grouping the hits within 100 ns into events. In case of the events in which two pixels fired in a module, only the pixel of the first interaction was considered. The pixel that is considered to have fired first is the one with lower deposited energy [22]. The difference in timestamps for events in which two pixels fired in opposite detectors can be seen in Figure 3, which represents plots of coincidence time spectra at the highest activity. The duration of the experiment was approximately one hour, and the length of acquisition at each of the 12 positions around the source ( $15^\circ$  apart)

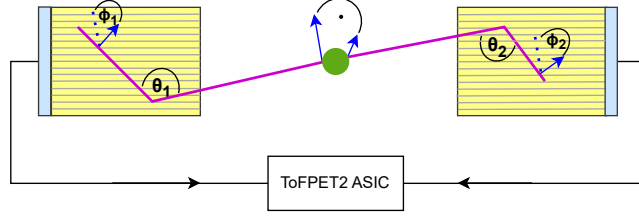


Figure 1: Simplified schematics of the experimental setup. The figure represents two segmented scintillating GAGG detector modules (in yellow) with SiPMs (in blue) in a coincidence measurement setup, read-out by the ToFPET2 ASIC system. The source (in green) emits two polarization-correlated annihilation photons (in purple) that undergo Compton scattering in their respective detector modules with Compton scattering angles  $\theta_{1,2}$  and azimuthal scattering angles  $\phi_{1,2}$ .

is given in Table 1.

### 2.3 Data selection and analysis

From the collected events, two types of events were selected: the single-pixel events, where each detector module fired with only one pixel in which the full energy ( $511 \text{ keV} \pm 3\sigma$ ) of the annihilation photon was deposited (i.e., photoelectric events), and events with two pixels fired per module with the sum of the deposited annihilation gamma-ray energies  $511 \text{ keV} \pm 3\sigma$ , with the minimum deposited energy of  $120 \text{ keV}$  per pixel. From the energies of the two pixels, Compton scattering angles  $\theta_{1,2}$  can be determined:

$$\theta = \arccos \left( \frac{m_e c^2}{E_{\text{px}_1} + E_{\text{px}_2}} - \frac{m_e c^2}{E_{\text{px}_2}} + 1 \right); \quad (3)$$

and from the topology of the detector modules, the azimuthal scattering angle  $\phi$ :

$$\phi = \text{atan} \left( \frac{\Delta y}{\Delta x} \right) \quad (4)$$

The final distribution of the difference of the azimuthal scattering angles  $\Delta\phi = \phi_1 - \phi_2$  is influenced by the distance of the two pixels that fired  $d = \sqrt{(\Delta x)^2 + (\Delta y)^2}$ , since the detector sensitivity has non-uniform acceptance for different event topologies, with events in which  $d$  is very large being almost negligible. This can be corrected ( $N_{\text{cor}}(\phi_1 - \phi_2)$ ) by normalizing the obtained distribution  $N(\phi_1 - \phi_2)$  of polarization-correlated events with events that are not recognized as correlated  $A_{\text{uncor}}(\phi_1 - \phi_2)$ :

$$N_{\text{cor}}(\phi_1 - \phi_2) = \frac{N(\phi_1 - \phi_2)}{A_{\text{uncor}}(\phi_1 - \phi_2)}. \quad (5)$$

---

Position	Acquisition time [s]	Total time [s]	Activity [MBq]
1	240	260	377.7
2	251	272	361.4
3	262	283	345.1
4	275	297	328.9
5	289	311	312.7
6	304	326	296.6
7	322	345	280.6
8	341	364	264.6
9	362	387	248.8
10	387	412	232.9
11	415	441	217.2
12	447	475	201.5

Table 1: The experiment was conducted by rotating the detector modules around the Ga-68 source, and the data were acquired in 12 positions. The length of acquisition at each position is given in the Table, as well as the total time (acquisition length with added time required for rotation to the next position) and activity of the Ga-68 source at the start of each acquisition.

This allows for the quantification of the polarimetric modulation factor  $\mu$  by fitting the Pryce-Ward formula to the obtained corrected distribution:

$$N_{cor}(\phi_1 - \phi_2) = M[1 - \mu \cos[2(\phi_1 - \phi_2)]], \quad (6)$$

as can be seen in Figure 2. The more in-depth description of the analysis process can be found in [10, 13, 23].

The coincidence time spectra for measurements at the highest activity (first position) are presented in Figure 3. The central peak was fitted by a Gaussian to determine its mean and standard deviation, and the data selected  $\pm 3\sigma$  from the peak (i.e.  $\sim \pm 2.5$  ns from the peak) was considered as a signal. The random background data was chosen as a  $6\sigma$  area at  $\pm 15\sigma$  ( $\sim \pm 8.5$  ns) distance from the calculated peak. After normalization of the random background data, the signal-to-random background (SBR) ratio is calculated by dividing the number of selected events in the signal and random background areas.

The data analysis was conducted in ROOT [24], with the optimization help from the GNU *parallel* command [25]. The obtained data was plotted in Python.

### 3 Results

We first investigated how the polarimetric modulation factor  $\mu$  behaves during the measurements with this experimental setup at high (approx. 200 MBq - 378

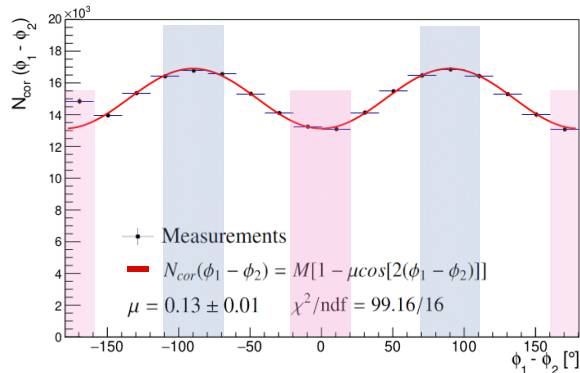
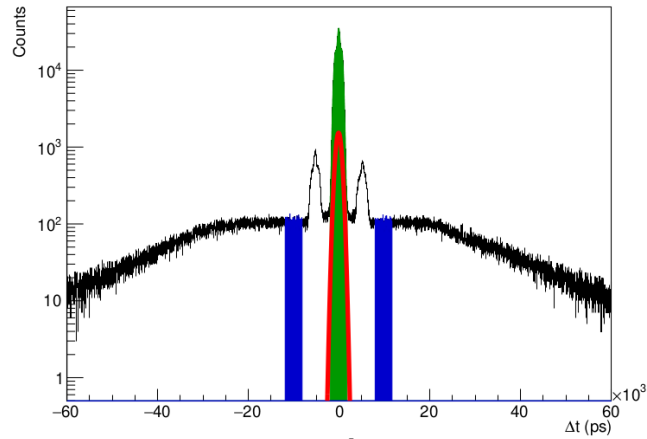


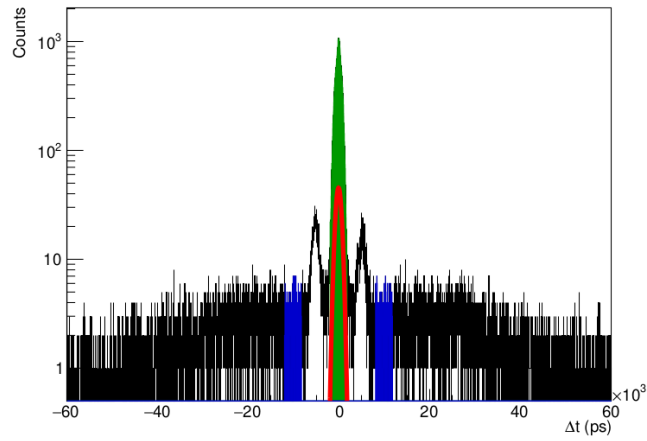
Figure 2: Acceptance corrected  $\phi_1$ - $\phi_2$  distribution at the sixth measurement position. The Compton scattering angle range was selected as  $\theta_{1,2} \in [72^\circ, 90^\circ]$ . The highlighted regions denote the azimuthal difference range of events selected for further analysis. The regions shaded in blue correspond to the  $\Delta\phi \in [70^\circ, 110^\circ]$ , and denote the highest probability of polarization correlations, while the regions shaded in pink, with  $\Delta\phi \in [-20^\circ, 20^\circ]$ , denote the lowest probability of two photons having correlated polarizations.

MBq) activity levels. The results are presented in Figure 4. We considered three different event topologies, where two pixels that fired in the selected Compton event could be the closest neighbors ( $d < 3.1$  mm) or if nearest neighbors are excluded ( $d > 4.6$  mm), and one in which the reconstructed Compton scattering angle  $\theta_{1,2} \in [60^\circ, 80^\circ]$  is less than optimal, but still potentially useful [7]. The selection of the polarization-correlated events of the topology where the closest neighbors are included exhibits  $\sim 28\%$  increase as the source activity declines from  $\sim 387$  MBq to  $\sim 200$  MBq. The selection of events in which the nearest neighbors are excluded shows higher  $\mu$  values than the events where they are included, which is to be expected [26, 23]. The selection also has a sensitivity gain of  $\sim 40\%$  at the end of the measurement. The event selection where  $\theta_{1,2} \in [60^\circ, 80^\circ]$  at these activities is not very feasible, since it showed low  $\mu$  values, at maximum  $\sim 8.5\%$ , and little gain following the decrease in source activity.

We also examined how the signal-to-random background ratios, calculated from the coincidence time spectra (Figure 3), varied across the source activity for single-pixel events and different selections of polarization-correlated events. In Figure 5, the events with polarization-correlated quanta at  $\theta_{1,2} \in [72^\circ, 90^\circ]$  and  $\Delta\phi \in [70^\circ, 110^\circ]$  (i.e. the blue-shaded area in Figure 2) exhibit higher random background suppression compared to the single-pixel events and the polarization-correlated events with the same  $\theta_{1,2}$  selection; however, the selection of the  $\Delta\phi$  that encompasses the valleys of the distribution (areas shaded in pink in Figure 2) shows the lowest reduction of the random background from the selected event types.



**a)**



**b)**

Figure 3: Coincidence time spectra for a) single-pixel (photoelectric) events and b) polarization-correlated Compton events. The signal (in green) is estimated as  $\pm 3\sigma$  from the mean calculated by the Gaussian fit (red curve) to the highest peak in each spectrum. The random background (in blue) is estimated as  $6\sigma$  area, removed from the calculated mean by  $\pm 15\sigma$ .

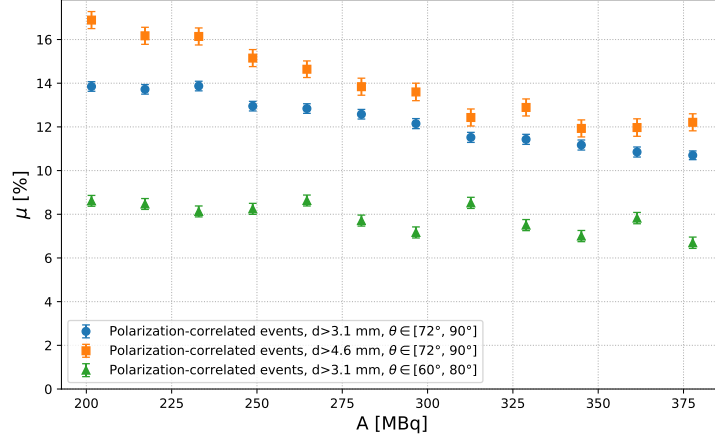


Figure 4: The measured values of the polarimetric modulation factor  $\mu$  exhibit higher values at lower source activity  $A$  levels for all selected event topologies.

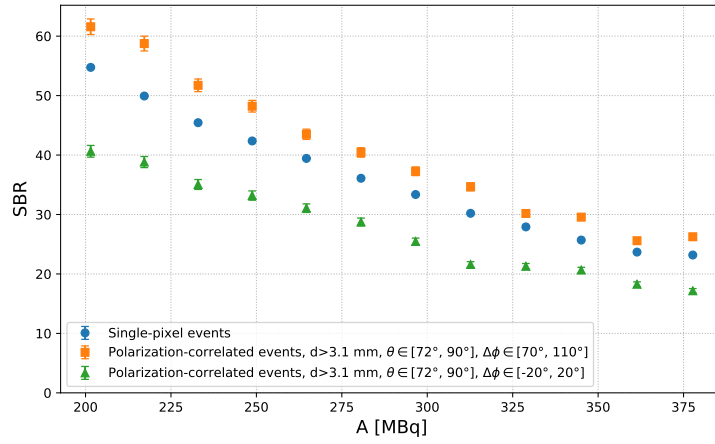


Figure 5: The signal-to-random background (SBR) ratio values across the different source activities  $A$  exhibit higher values in case of polarization-correlated events selected for optimal Compton scattering angles  $\theta_{1,2} \in [72^\circ, 90^\circ]$  and highest correlation probability  $\Delta\phi \in [70^\circ, 110^\circ]$ .

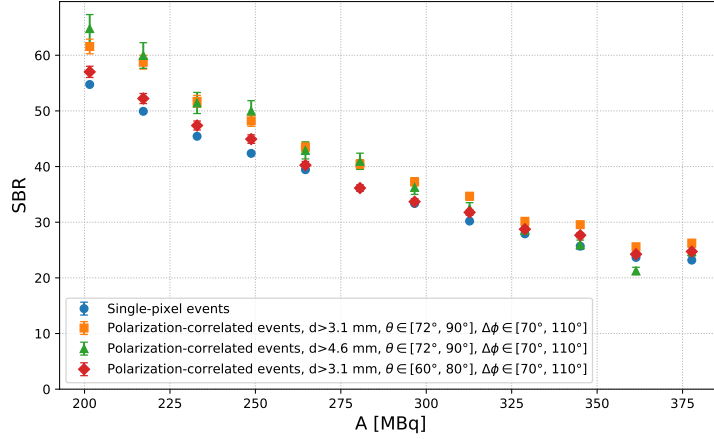


Figure 6: The SBR of different polarization-correlated events' topologies compared to the single-pixel events across the source activities  $A$ . The choice of the event topology (i.e., the choice of the distance  $d$  between the pixels, and the selection of the Compton scattering angle  $\theta$ ) influences the quantity of the random background reduction at different source activities.

In addition, we explored how the SBR values of different event topologies vary across the source activities. The results can be seen in Figure 6. It can be observed that the differences in background reduction between different event topologies, such as selection of the distance between the pixels, as well as selection of the Compton scattering angle  $\theta$ , are narrowing with the increase of the source activity.

The SBR values were also influenced by the sensitivity of the detector setup on measurements of the polarization correlated annihilation photons, described by the polarimetric modulation factor  $\mu$ . This is evident in Figure 7, where the selections of the azimuthal angle difference  $\Delta\phi \in [70^\circ, 110^\circ]$  (blue areas from the Figure 2) illustrate that with the increase of  $\mu$ , the SBR values increase as well, signaling higher random background reduction. The difference in values at the beginning of the measurement (i.e. the source activity  $\sim 378$  MBq) and end (the source activity of  $\sim 200$  MBq) is  $\sim 50\%$ .

The ratios of the SBR values obtained from the coincidence time spectra for selected polarization-correlated events to the SBR values for single-pixel events remain consistent during the experiment, and their value is approximately 1.23, meaning the polarization-correlated events have  $\sim 23\%$  higher values than single-pixel events. These results can be seen in the Figure 8, for both source activity levels and the values of the polarimetric modulation factor  $\mu$ .

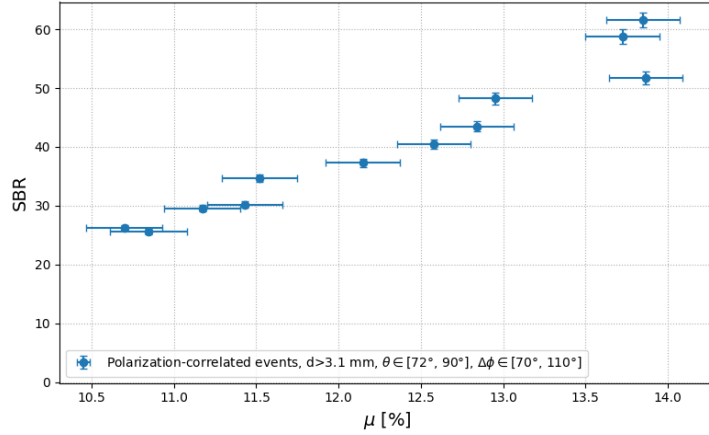
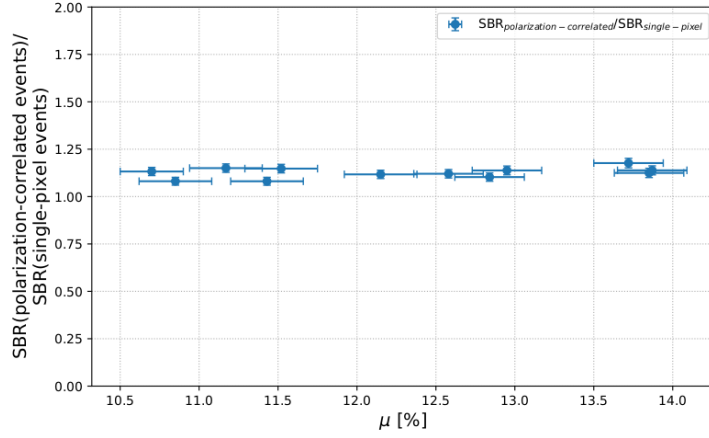


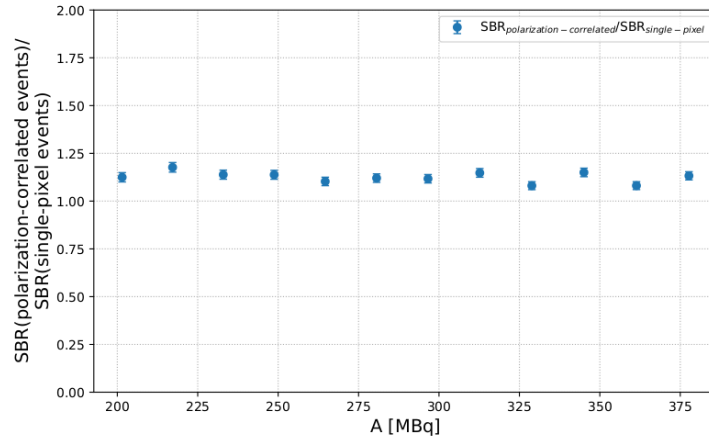
Figure 7: The SBR values of events with measurements of the polarization-correlated annihilation quanta increase with the polarimetric modulation factor  $\mu$ , here obtained for the events with Compton scattering angle  $\theta_{1,2} \in [72^\circ, 90^\circ]$ .

## 4 Discussion and conclusion

The measurements of the polarization correlations of the annihilation photons could potentially be useful in suppression of the random coincidence events in PET imaging, since they lack this type of correlations. During the experiment with the Ga-68 source (with activity varying from  $\sim 200$  MBq to  $\sim 378$  MBq), we observed that the polarimetric modulation factor  $\mu$  has changed with the source activity (Figure 4), as it increased  $\sim 20\%$  in value during the experiment for the polarization-correlated events with Compton scattering angle  $\theta_{1,2} \in [72^\circ, 90^\circ]$  and azimuthal angle difference  $\Delta\phi \in [70^\circ, 110^\circ]$ . This could imply that the activity of the annihilation source could be of potential influence on the signal-to-random background suppression in measurements of the annihilation photons, as the SBR is increasing with lowering activity levels, too (Figures 5 and 6), with the minimum of  $\sim 28\%$  higher values for SBR of polarization-correlated events with Compton scattering angle  $\theta_{1,2} \in [72^\circ, 90^\circ]$  and azimuthal angle difference  $\Delta\phi \in [70^\circ, 110^\circ]$ , compared to SBR of the single-pixel events. The decrease in random background suppression with activity that we observed, as well as the lower values of the polarimetric modulation factor  $\mu$  could potentially suggest there might be a limit to the rate of accepted events in the case of very high source activities in this and other comparable experimental settings, as the ratio of the SBR of the polarization-correlated events and the SBR of the single-pixel events remains constant with levels of source activity and values of the polarimetric modulation factor  $\mu$ , with SBR of the polarization-correlated events 23% higher than the SBR of the single-pixel events. The SBR of the events with polarization correlations selected from the peaks (area shaded in blue) in Figure 2 exhibit  $\sim 50\%$  increase in value with the  $\sim 30\%$  rise in the



**a)**



**b)**

Figure 8: The ratios of the SBR values obtained with the polarization-correlated events and single-pixel events stay consistent across varying factor  $\mu$  (in a)), calculated for the optimal Compton scattering angles  $\theta_{1,2} \in [72^\circ, 90^\circ]$  and azimuthal angle difference  $\Delta\phi \in [70^\circ, 110^\circ]$ , and source activity A (in b)).

---

value of the polarimetric modulation factor  $\mu$ . This could potentially be useful for the optimization of the experiment setup, since  $\mu$  will depend on the topology of the selected events (for example, the distance between the pixels that fired in a Compton event), the medium in which the source is contained, as well as the activity of the source.

## Acknowledgements

This work was supported by the “Research Cooperability” Program of the Croatian Science Foundation, funded by the European Union from the European Social Fund under the Operational Programme Efficient Human Resources 2014–2020, grant number PZS-2019-02-5829. This work was also supported by the Croatian Science Foundation under the project number IP-2022-10-3878.

## References

- [1] Dirac P. The quantum theory of the electron. *Proc. R. Soc. Lond. A*, 117:610–624, 1928.
- [2] Bass SD, Mariazzi S, Moskal P, and Stepien E. Colloquium: Positronium physics and biomedical applications. *Reviews of Modern Physics*, 95:021002, 2023.
- [3] Moskal P. Positron Emission Tomography Could Be Aided by Entanglement. *Physics*, 17:138, September 2024.
- [4] M. H. L. Pryce and J. C. Ward. Angular correlation effects with annihilation radiation. *Nature*, 160:4065, 1947.
- [5] Kuncic Z, McNamara A, Wu K, and Boardman D. Polarization enhanced x-ray imaging for biomedicine. *Nuclear Instruments and Methods in Physics Research Section A: Accelerators, Spectrometers, Detectors and Associated Equipment*, 648:S208–S210, 2011.
- [6] McNamara A, Toghyani M, Gillam JE, Wu K, and Kuncic Z. Towards optimal imaging with PET: An in silico feasibility study. *Physics in Medicine and Biology*, 59:7587–7600, 2014.
- [7] Toghyani M, Gillam JE, McNamara A, and Kuncic Z. Polarisation-based coincidence event discrimination: An in silico study towards a feasible scheme for Compton-PET. *Physics in Medicine and Biology*, 61:5803–5817, 2016.
- [8] Watts DP, Bordes J, Brown JR, Cherlin A, Newton R, Allison J, Bashkanov M, Efthimiou N, and Zachariou NA. Photon quantum entanglement in the MeV regime and its application in PET imaging. *Nature Communications*, 12:2646, 2021.

- 
- [9] Kim D, Rachman AN, Taisei U, Uenomachi M, Shimazoe K, and Takahashi H. Background reduction in PET by double Compton scattering of quantum entangled annihilation photon. *Journal of Instrumentation*, 18:P07007, 2023.
- [10] Makek M, Bosnar D, Pavelić L, Šenjug P, and Žugec P. Single-layer Compton detectors for measurement of polarization correlations of annihilation quanta. *Nuclear Instruments and Methods in Physics Research Section A: Accelerators, Spectrometers, Detectors and Associated Equipment*, 958:162835, 2020.
- [11] Kumar D, Sharma S, and Moskal P On behalf of J-PET collaboration. Investigating quantum entanglement of high-energy photons from positron annihilation in a porous medium. *Journal of Physics: Conference Series*, 3029(1):012006, June 2025.
- [12] Romanchek GR, Shoop G, Kupinski MA, Kuo PH, King M, Furenlid LR, and Abbaszadeh S. Investigation of quantum entanglement information for  $\beta^+\gamma$  coincidences. *Bio-Algorithms and Med-Systems Special Issue*, pages 27–34, 2024.
- [13] Kožuljević AM, Bokulić T, Grošev D, Kuncic Z, Parashari S, Pavelić L, and Makek M. Investigation of the spatial resolution of PET imaging system measuring polarization-correlated Compton events. *Nuclear Instruments and Methods in Physics Research Section A: Accelerators, Spectrometers, Detectors and Associated Equipment*, 1068:169795, 2024.
- [14] Moskal P, Kumar D, Sharma S, Yitayew Beyene E, Chug N, Coussat A, Curceanu C, Czerwiński E, Das M, Dulski K, Gorgol M, Jasińska B, Kacprzak K, Kaplanoglu T, Kapłon L, Kozik T, Lisowski E, Lisowski F, Mryka W, Niedźwiecki S, Parzych S, del Rio EP, Rädler M, Skurzok M, Stepień EL, Tanty P, Tayefi Ardebili K, and Valsan Eliyan K. Nonmaximal entanglement of photons from positron-electron annihilation demonstrated using a plastic PET scanner. *Science Advances*, 11(18):eads3046, 2025.
- [15] Caradonna P. Kinematic analysis of multiple Compton scattering in quantum-entangled two-photon systems. *Annals of Physics*, 470:169779, 2024.
- [16] Caradonna P. Compton scattering mediated by quantum entanglement. *Phys. Rev. A*, 111:053708, May 2025.
- [17] Caradonna P and Shimazoe K. Entanglement, steering, and separability in Compton-scattered annihilation photons. *Phys. Rev. A*, 112:032413, 2025.
- [18] Hiesmayr BC, Krzemień W, and Bała M. Quantum error channels in high energetic photonic systems. *Scientific Reports*, 14:9672, 2024.

- 
- [19] Bała M, Krzemień W, Hiesmayr B, Baran J, Dulski K, Klimaszewski K, Raczyński L, Shopa RY, and Wiślicki W. Probing arbitrary polarized photon pairs undergoing double Compton scatterings by a dedicated mc simulator validated with experimental data. *The European Physical Journal C*, 85:1115, 2025.
- [20] S. Parashari *et al.* Optimisation of detector modules for measuring gamma-ray polarization in Positron Emission Tomography. *Nuclear Instruments and Methods in Physics Research Section A: Accelerators, Spectrometers, Detectors and Associated Equipment*, 1040:167186, 2022.
- [21] Di Francesco A, Bugalho R, Oliveira L, Pacher L, Rivetti A, Rolo M, Silva J C, Silva R, and Varela J. TOFPET2: A high-performance ASIC for time and amplitude measurements of SiPM signals in time-of-flight applications. *Journal of Instrumentation*, 11:C03042, 2016.
- [22] Kožuljević AM, Bosnar D, Kuncic Z, Makek M, Parashari S, and Žugec P. Study of multi-pixel scintillator detector configurations for measuring polarized gamma radiation. *Condensed Matter*, 6:43, 2021.
- [23] S. Parashari *et al.* Measurement of angular correlations of Compton-scattered gamma quanta from positron annihilation using GAGG:Ce scintillator matrices with single-side readout. *Journal of Instrumentation*, 17:C09007, 2022.
- [24] Brun R and Rademakers F. ROOT - An Object Oriented Data Analysis Framework. *Nucl. Instrum. Methods Phys. Res. A*, 389:81–86, 1997.
- [25] O. Tang. GNU Parallel 20210822 ('Kabul'). *Zenodo*, 2022.
- [26] Makek M, Bosnar D, Gačić V, Pavelić L, Šenjug P, and Žugec P. Performance of scintillation pixel detectors with MPPC read-out and digital signal processing. *Acta Physica Polonica B*, 48(10):1721–1726, 2017.